Preformation of alpha-clusters in alpha-decay

IOP Conf. Series: Journal of Physics: Conf. Series **863** (2017) 012011 doi:10.1088/1742-6596/863/1/012011

Preformation of alpha-clusters in alpha-decay

R G Lovas

MTA Institute for Nuclear Research, PO Box 51, H–4001 Debrecen, Hungary

Abstract. Comprehensive cluster-model analyses of all decay cases show that the probability of clustering in most α-decaying states is close to unity. Although early shell-model results for the preformation probability grossly undershot this value and the α-decay width accordingly, more recent sophisticated microscopic structure calculations are in agreement with this observation, except that of a complex-energy shell model. I review the relavant shell model calculations in an attempt to pinpoint the crucial ingredients, which are likely to be responsible for this disagreement.

1. Introduction

Before 1975 it was generally assumed that α preformation in the parent nucleus is meagre. This belief was primarily based on contemporary shell-model calculations. But with the shell-model bases enlarged, the estimates for clustering increased [1, 2]. In particular, the ^{208}Pb+α component in the ^{212}Po g.s. has been found to be 0.3. At the same time, the widths of all favoured α-decays were reproduced in an extreme cluster model, providing evidence for strong clustering in α-decaying states [3, 4]. The consistency of appreciable clustering with realistic width has been confirmed by a nuclear-matter-motivated approach [5]. Thus there seemed to be an accord among various results.

In the last cluster conference [6], however, it was reported that the decay width of ^{212}Po is reproduced in a shell model that yields a much smaller value for clustering (about 1%) than the the classical microscopic calculations (> 0.1). This contradiction requires a review of the intricacies and pitfalls in the advanced shell models. My attention is focussed on the ^{212}Po$\rightarrow^{208}$Pb+α system, in which ^{212}Po is assumed to consist of a passive ^{208}Pb core and four active valence nucleons.

2. Clustering and decay properties

In a state $\Psi^{\rm P}$ of a parent nucleus P the formation of a daughter+α-particle (D+α) pair, described by wave functions $\Phi^{\rm D}$ and Φ^{α}, is characterized by $g(\mathbf{R}) = \langle \mathcal{A}\{\Phi^{\rm D}\Phi^{\alpha}\delta(\mathbf{R}-\mathbf{R}_{\alpha{\rm D}})\}|\Psi^{\rm P}\rangle$, where the interfragment antisymmetrizing operator $\mathcal{A}$ acts on both the intrinsic coordinates and the relative coordinate $\mathbf{R}_{\alpha{\rm D}}$ of the fragments. This formation amplitude and the spectroscopic factor $S = \int d\mathbf{R}|g(\mathbf{R})|^2$ had been attributed probability meaning. It was recognized by Fliessbach [7] that this cannot be correct. He introduced a proper probability amplitude $G(\mathbf{R})$ and probability $\mathcal{S}$ as

$$G(\mathbf{R}) = \mathcal{N}^{-1/2} g(\mathbf{R}), \qquad \mathcal{S} = \int d\mathbf{R}|G(\mathbf{R})|^2,$$

where $\mathcal{N}$ is a resonating-group-like norm operator, whose kernel is

$$N(\mathbf{R},\mathbf{R}') = \langle \mathcal{A}\{\Phi^{\rm D}\Phi^{\alpha}\delta(\mathbf{R}-\mathbf{R}_{\alpha{\rm D}})\}|\mathcal{A}\{\Phi^{\rm D}\Phi^{\alpha}\delta(\mathbf{R}'-\mathbf{R}_{\alpha{\rm D}})\}\rangle.$$

For a pure cluster state, $\mathcal{S} = 1$ as it should be, while $S \neq 1$. In fact, for a heavy two-cluster system, $S \ll \mathcal{S} < 1$ since the Pauli suppression in $g(\mathbf{R})$ is 'overdosed'. (For recent examples, see Ref. [8].) The former misinterpretation of S as a clustering probability contributed to the underrating of clustering. For a spherical nucleus the decay width is usually calculated from the tail of the amplitude $g(\mathbf{R})$ or $G(\mathbf{R})$. The decay width is then $\Gamma = 2P(R_0)(\hbar^2/2\mu R_0)g^2(R_0)$, where $g(R)$ is the radial factor

of $g(\mathbf{R}) = (g(R)/R)Y_{lm}(\hat{R})$, l is the relative angular momentum, μ is the reduced mass and P is the penetrability. It is important that $R_0 = |\mathbf{R}_0|$ should be in the asymptotic region, i.e., it should be larger than the range of $\mathcal{A}$ and of the nuclear force between the fragments. Then in that region $g(\mathbf{R}_0) = G(\mathbf{R}_0)$, and P is the Coulomb penetrability.

3. Improved shell models

The standard shell model is distinguished from other microscopic models by its being unbiassed for clustering. Its bases consist of all configurations of the lowest-lying s.p. states. The low-lying s.p. states, however, do not stretch out far from the centre, which makes it difficult to produce a $g(R)$ that is realistic in the asymptotic region.

3.1. Cluster-configuration shell model (CCSM)

If the core is taken infinitely heavy, the shell model basis can be complemented by states of the form of $\mathcal{A}\{\Phi^\alpha_{\mathbf{s}}\Phi^{\mathrm{D}}\}$, where $\Phi^\alpha_{\mathbf{s}}$ is a Slater determinant of shifted 0s orbits $\phi^{(\beta)}_{\mathbf{s}}(\mathbf{r}) \propto \exp[-\frac{1}{2}\beta(\mathbf{r}-\mathbf{s})^2]\chi$, where χ is a spin-isospin state. A c.m. factor can then be separated from the determinant $\Phi^\alpha_{\mathbf{s}}$

$$\mathcal{A}\{\Phi^\alpha_{\mathbf{s}}\Phi^{\mathrm{D}}\} \propto \mathcal{A}\{\exp[-2\beta(\mathbf{R}_{\alpha\mathrm{D}} - \mathbf{s})^2]\Phi^\alpha\Phi^{\mathrm{D}}\},$$

where Φ^α is an intrinsic alpha-particle wave function. This shows that the shifted Gaussian orbits $\phi^{(\beta)}_{\mathbf{s}}$ give rise to basis elements that contain two-cluster states. (These are to be projected to angular momentum 0.) The antisymmetrization eliminates the components of the s.p. Gaussians that are not orthogonal to the orbits occupied in the core. This makes it possible to get rid of the core so as to incorporate the core effects in a projection operator $\mathcal{P}$, which projects off all the core orbits [9].

The model with one major valence shell (538 basis states) and 30 to 40 shifted Gaussians with well-positioned centres $\mathbf{s}$ and $R_0 > 10$ fm yield Γ=1.2×10^{-15} MeV to 1.6×10^{-15} MeV, thus reproducing the experimental value of Γ=1.5×10^{-15} MeV.

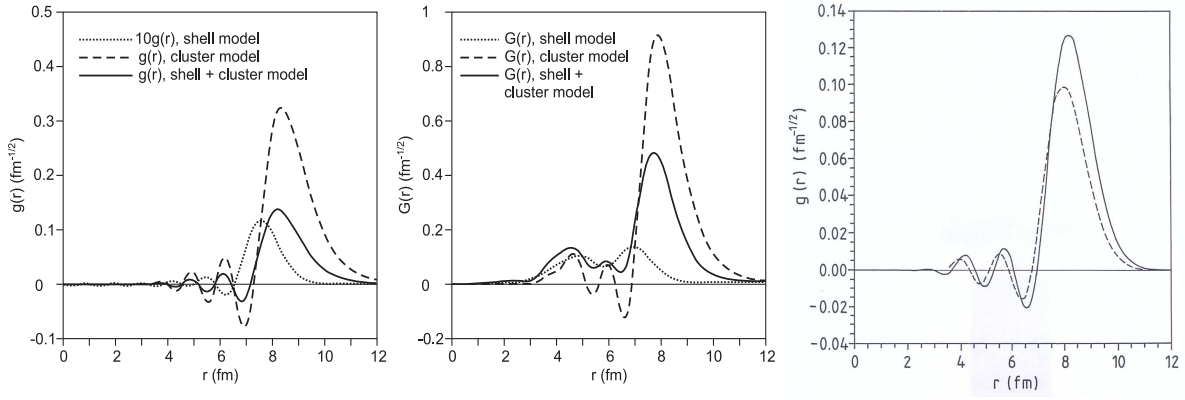

Figure 1. Left and middle panels: $g(r)$ and $G(r)$ for the ^{212}Po=^{208}Pb+α decay in the thee models given in the legends [10]. Right panel: $g(r)$ in the SSM (dashed line; see Sect. 3.2) and in the CCSM (full line) [11]

The $g(r)$ and $G(r)$ produced by the shell model with and without cluster configurations and by the cluster configurations alone are shown on the left and middle panels of Fig. 1. The $g(R)$ of the CCSM is an order of magnitude larger and stretches out more than that of the ordinary shell model. All $g(R)$ oscillate around 0 like ordinary wave functions, with 11 or 12 nodes. The curves $G(R)$, on the contrary, have arkward shapes, except for that of the pure cluster model. This bears out the tendency observed in other works [1, 12, 13, 14]. To explain this behaviour, let us expand the amplitudes in terms of the complete orthonormal set of the norm-operator eigenfunctions $\{\varphi_\nu\}$ [15]:

$$g^{\rm sh}(\mathbf{R}) = \sum_\nu n_\nu^{1/2} \langle \Xi_\nu | \Phi^{\rm sh} \rangle \varphi_\nu(\mathbf{R}), \quad G^{\rm sh}(\mathbf{R}) = \sum_\nu \langle \Xi_\nu | \Phi^{\rm sh} \rangle \varphi_\nu(\mathbf{R}),$$
$$g^{\rm cl}(\mathbf{R}) = \sum_\nu n_\nu \langle \varphi_\nu | \phi^{\alpha {\rm D}} \rangle \varphi_\nu(\mathbf{R}), \quad G^{\rm cl}(\mathbf{R}) = \sum_\nu n_\nu^{1/2} \langle \varphi_\nu | \phi^{\rm rel} \rangle \varphi_\nu(\mathbf{R}).$$

Here $\phi^{\alpha {\rm D}}$ stands for the relative-motion function in the cluster-model or in the cluster-model term of the CCSM wave function, n_ν are the eigenvalues of the norm operator ($\mathcal{N}\varphi_\nu = n_\nu \varphi_\nu$), Ξ_ν are normalized two-cluster states in which the relative motion function is φ_ν (that is $\Xi_\nu = n_\nu^{-1/2} \mathcal{A}\{\Phi^{\rm D}\Phi^\alpha \varphi_\nu\}$), and $\Phi^{\rm sh}$ is the shell-model wave function or the shell-model term of the CCSM. Both $\langle \Xi_\nu | \Phi^{\rm sh} \rangle$ and $\langle \varphi_\nu | \phi^{\rm rel} \rangle$ are overlaps between normalized functions, and, for small ν values, both the bra and the ket functions are appreciable in the nuclear volume. The first eigenvalue $n_0 \approx 10^{-7}$ and $n_\nu \longrightarrow 1$ monotonously (see the left panel of Fig. 2). Since φ_ν have $\nu = 0, 1, 2, \ldots$ internal nodes and $n_\nu < 0.1$ for $\nu \leq 11$, the functions $g^{\rm sh}$, $g^{\rm cl}$ and $G^{\rm cl}$ are approximately orthogonal to all φ_ν up to $\nu = 11$, hence they are bound to have at least 12 nodes. No such statement holds for $G^{\rm sh}$, since its expansion contains no n_ν. That explains the nodal behaviours of the functions in Fig. 1.

3.2. Stochastic shell model (SSM)

A shifted Gaussian basis may be said to be biassed for clustering, although the variational principle underlying the shell model reduces the bias. An unbiassed shell-model of tractable size can be set up by the use of the stochastic variational method with Gaussian orbits [16]. This is a powerful method for the description of few-body systems, such as the five-body system of ^{212}Po=^{208}Pb+p+p+n+n. A Gaussian orbit of parameter μ projected to orbital angular momentum l looks like $u_l^\mu(r) \propto r^l \exp(-\frac{1}{2}\mu r^2)$, and in the basis states the angular momenta are to be coupled according to the following pattern: $[[[l_\pi \frac{1}{2}]_{j_\pi}][l'_\pi \frac{1}{2}]_{j'_\pi}]_J [[l_\nu \frac{1}{2}]_{j_\nu}][l'_\nu \frac{1}{2}]_{j'_\nu}]_J]_0$. These proton ($\pi$) and neutron ($\nu$) quantum numbers should run over all values that yield reasonable configurations over the core, with $J = 0, 1, 2, \ldots$ The trial function is constructed term by term from among many functions of randomly selected parameters $\mu_1, \ldots, \mu_4$. A term is adopted in the basis if it lowers the energy sufficiently when added to the trial function constructed in the previous step [16]. For the case of ^{212}Po [11], convergence was achieved with about 120 configurations and basis dimension about 400, at energy $E = -19.25$ MeV (experiment: $E = -19.35$ MeV). With the same interaction, the CCSM and the conventional shell model produce $E = -19.18$ MeV and $E = -18.96$ MeV, respectively. The SSM α-formation amplitude $g(r)$ is compared with that of the CCSM on the right panel of Fig. 1. There is a factor of 2 between the spectroscopic factors, and a factor of 3 between the widths.

It is remarkable that the SSM nearly reproduces the CCSM result with an ordinary shell-model basis, which is optimized solely for energy, thus is certainly unbiassed for clustering. This nice work [11] has been mostly overlooked hitherto.

3.3. Complex-energy shell model (CSM)

The novelty in this approach is the inclusion, in the basis, of s.p. resonances treated as complex-energy eigenstates with outgoing-wave asymptotics [17] (2 neutron and 11 proton resonances). The width is calculated as $\Gamma = \mathcal{S}\Gamma^{\rm s.p.}$, where $\Gamma^{\rm s.p.}$ is the width in a single-α-particle model. The $G(R)$ implicit in $\mathcal{S}$ is to be calculated via $G(\mathbf{R}) = \mathcal{N}^{-1/2} g(\mathbf{R})$, where $\mathcal{N}^{-1/2} = \sum_\nu |\varphi_\nu\rangle n_\nu^{-1/2} \langle \varphi_\nu|$. (There are no zero eigenvalues.) The resulting $g(R)$ has no internal nodes, while $G(R)$ has 10. Thus these functions do not follow the nodal behaviour shown to be generally valid in Sect. 3.1. They come close to zero at about 10 fm as much as the $g(R)$ and $G(R)$ of the CCSM do at 12 fm, thus their range may be said to be 2 fm shorter, and no wonder that they produce 30 times smaller clustering probability, and the tail of $G(R)$ would predict a width smaller by a factor of 36. This result breaks the trend of $S \ll \mathcal{S}$ as well; in fact, $\mathcal{S} < S$. This suggests that there is something the matter with the values of n_ν.

What is surprising is that, despite the unphysical shapes of $g(R)$ and $G(R)$ and despite their too short tails, the width calculated from $\Gamma = \mathcal{S}\Gamma^{\rm s.p.}$ is perfect. As is shown in Fig. 2b, the eigenvalues strongly depend on the basis used for their calculation. The most inaccurate small n_ν were discarded on the grounds that they are spurious. They are certainly not spurious [18], but their inaccuracy and

omission do not influence the tail of $G(R)$, hence the reasonability of the Γ value that is extracted from the tail.

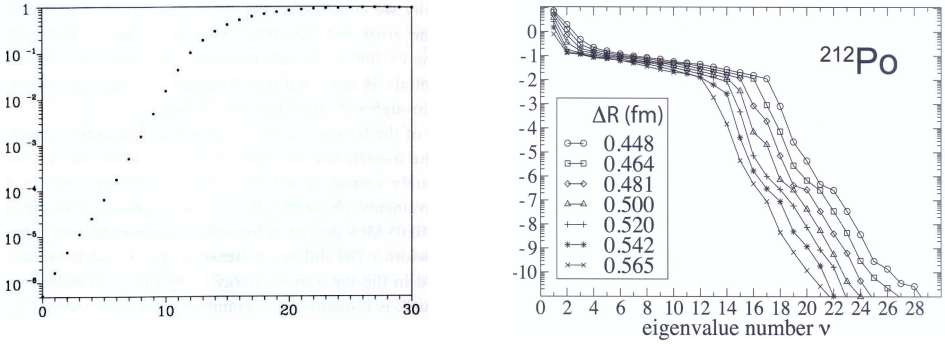

Figure 2. Eigenvalues n_ν of the norm kernel. (a) Left panel: Ref. [9]; (b) right panel: Ref. [6] in reverse sequence; the different symbols distinguish between results with different bases [6].

4. Conclusion

Apart from some aspects of the CSM [6], the shell-model description of α-decay is well understood. The motivation of the CSM was to include the continuum in the basis. The continuum has often been referred to as an important missing ingredient in the usual descriptions of the decay. However, the continuum can be well represented by a set of discrete states. In fact, it is represented by discrete (resonance) states even in Ref. [6]. Moreover, what is included there is not the four-particle continuum but some part of the s.p. continuum. The α-decay width is borne by the tail of the wave function in the four-particle channel, and there is a tremendous difference between the single-nucleon and the four-nucleon continua. The tail behaviour can be made realistic by long-tailed basis functions in the four-particle channel like in the CCSM. The Gaussian wave packets used there are predominantly combinations of four-particle continuum states, thus the continuum states are in fact not missing.

If the formula $\Gamma = \mathcal{S}\Gamma^{\text{s.p.}}$ is used to calculate Γ, it may be enough for the wave function of the single-α-particle model to show the correct tail behaviour, but the clustering probability can only be correct if $G(R)$ is correct at least up to and including the last large peak.

References

[1] Tonozuka I and Arima A 1979 *Nucl. Phys.* A **323** 45
[2] Lovas R G, Liotta R J, Insolia A, Varga K and Delion D S 1998 *Phys. Rep.* **294** 265
[3] Buck B, Merchant A C and Perez S M 1990, *Phys. Rev. Lett.* **65** 2975
[4] Buck B Merchant A C and Perez S M 1993 *At. Data Nucl. Data Tables* **54** 53; Ohkubo S *et al.* 1998 Prog. Theor. Phys. Suppl. **132** 1–228; Buck B, Merchant A C, Perez S M and Seals H E 2005 *J. Phys.* G **31** 1499; Ren Y and Ren Zh 2012 *Phys. Rev.* C **85** 044608; Xu F R, Wang S M, Lin Z J and Pei J C 2013 *J. Phys.: Conf. Ser.* **436** 012064
[5] Xu Ch, Ren Zh, Röpke G, Schuck P, Funaki Y, Horiuchi H, Tohsaki A, Yamada T and Zhou B 2016 *Phys Rev* C **93** 011306(R) Horiuchi H 1977 Prog. Theor. Phys. Suppl. **62** 90
[6] Id Betan R 2013 *J. Phys.: Conf. Ser.* 012061; Id Betan R and Nazarewicz W 2012 *Phys. Rev.* C **86** 034338
[7] Fliessbach T 1975 *Z Phys* A **272** 39
[8] Volya A and Tchuvil'sky Y M 2015 *Phys. Rev.* C **91** 044319
[9] Varga K, Lovas R G and Liotta R J 1992 *Nucl. Phys.* A **550** 421
[10] Varga K, Lovas R G and Liotta R J 1992 *Phys. Rev. Lett.* **69** 37
[11] Varga K and Liotta R J 1994 *Phys. Rev.* C **50** R1292
[12] Fliessbach T and Mang H J 1976 *Nucl. Phys.* A **263** 75
[13] Okabe S 1989 Suppl. J. Phys. Soc. Jpn. **58** 516
[14] Okabe S and Fliessbach T 1984 *Phys. Lett.* B **144** 5
[15] Lovas R G 2016 *Phys. Rev.* C **93** 069801
[16] Varga K, Suzuki Y and Lovas R G 1994 *Nucl. Phys.* A **571** 447
[17] Berggren T 1968 *Nucl. Phys.* A **109** 265
[18] Horiuchi H 1977 Prog. Theor. Phys. Suppl. **62** 90